

# Amine-Functionalization of the Nanotitanate ETS-2

Brenden Tanchuk, James A. Sawada, and Steven M. Kuznicki

Dept. of Chemical and Materials Engineering, University of Alberta, Edmonton, Alberta, T6G 2V4, Canada

DOI 10.1002/aic.14205

Published online August 9, 2013 in Wiley Online Library (wileyonlinelibrary.com)

*A series of nonporous, amine-functionalized sodium titanates was prepared and the thermal and adsorptive behavior of the samples were characterized. Engelhard titanosilicate 2 was chosen as a substrate for its high surface area (~300 m<sup>2</sup>/g), native surface hydroxyl concentration, and lack of microporosity; eliminating the risk of fouling the adsorbent under certain process conditions. Aminosilanes containing a single (N1), two (N2), and three (N3) amine groups were chemically grafted to the surface of the substrate and the adsorption capacity for CO<sub>2</sub> measured through thermogravimetry-mass spectroscopy (TG-MS) desorption, volumetric adsorption, and gravimetric adsorption/desorption cycling. The N3 sample displayed complete monolayer coverage and was capable of adsorbing five times as much atmospheric CO<sub>2</sub> as the N1 sample. Testing under anhydrous conditions only engages the primary amine on the tether and the data consistently suggests a correlation between amine utilization and the proportion of monolayer coverage for these adsorbents. © 2013 American Institute of Chemical Engineers AIChE J, 59: 4727–4734, 2013*

**Keywords:** carbon dioxide, adsorption, amine grafting, Engelhard titanosilicate 2, nonporous

## Introduction

Since 1990s attention has focused on the increasing emission of carbon dioxide worldwide and on how this is affecting global temperatures and climate. The production of carbon dioxide is increasing at a rate of ~500 million tones per year.<sup>1</sup> Many studies have been carried out that have investigated technological solutions to this issue. One proposed solution that has garnered attention in the past decade is the concept of post combustion capture (PCC) of carbon dioxide combined with sequestration. A PCC system uses a separation process to remove and concentrate carbon dioxide from a flue gas stream. The concentrated carbon dioxide is then compressed and permanently sequestered.

Despite being a mature technology, liquid amine scrubbers are an imperfect solution for PCC. The cost and complexity of liquid amine systems and the environmental concerns surrounding amine volatilization have driven a materials development effort whose goals have been to replace liquid contractors with packed-bed towers containing dry adsorbents found in temperature swing adsorption and pressure swing adsorption systems.<sup>2–5</sup> The work has been directed to maintain the high specificity of the amine functionality toward dilute CO<sub>2</sub> in the presence of water vapor while simultaneously taking advantage of the process simplification offered by columns filled with beaded adsorbents.

Conventional molecular sieves<sup>5–8</sup> and associated materials such as activated carbons,<sup>9,10</sup> silica gel,<sup>11,12</sup> and activated alumina<sup>13,14</sup> can have appealing CO<sub>2</sub> capacity per gram of adsorbent but their sensitivity to water precludes them from being considered for streams containing high levels of

humidity. In the case of zeolite molecular sieves, any measurable amount of moisture will progressively poison the sieve over time, whereas amorphous adsorbents such as silica gel and activated alumina are inefficient as, being effective desiccants, favor water over CO<sub>2</sub>. Conventional activated carbons have a balance of properties which would seem to make them ideal for CO<sub>2</sub> capture from air but such materials suffer from capillary condensation when the relative humidity in the stream exceeds about 40–50% relative humidity (RH) at which point the pore space floods with water which must be rejected before CO<sub>2</sub> can be adsorbed. The implementation hurdles associated with conventional adsorbents have directed efforts toward pairing the chemical specificity and water tolerance of the amine chemistry with a porous, solid support that can be formed into macroscopic particles and packed into a column.

One avenue of investigation seeks to immobilize the amine by using a solid adsorbent as a vessel to hold an amine fluid.<sup>15,16</sup> Such schemes pair a chemically stable micro or mesoporous solid with an amine fluid matched to the steric considerations and the pore volume of the adsorbent. The adsorptive force within the pores exerted on the amine reduces its vapor pressure compared to the neat liquid. The vapor pressure of the amine, while lower than the bulk liquid, is finite and amine vapor will leach into the regeneration stripping stream. These cyclic losses reduce the capacity of the bed over time and, unlike bulk liquid systems where additional amine may be added to replace losses, a packed bed column cannot be easily replenished to increase capacity.

Another method for immobilizing the amine is to chemically graft an amine functionality to the surface of a solid. Such schemes eliminate the vapor losses associated with physically adsorbed amines by covalently bonding the organic chain to the surface of the material. Traditional amine fluids such as monoethanolamine (MEA) and

Correspondence concerning this article should be addressed to S. M. Kuznicki at [steve.kuznicki@ualberta.ca](mailto:steve.kuznicki@ualberta.ca).

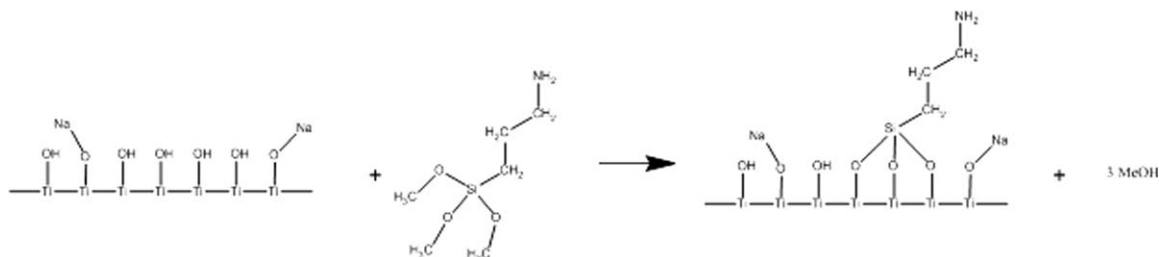


Figure 1. Schematic of grafting reaction of (3-aminopropyl)trimethoxysilane to ETS-2 surface.

diethanolamine (DEA) lack the chemical functionality to graft them to the surface of a solid and thus surrogate materials have been identified. Trimethoxyaminosilanes have both a chemical function that will interact and bond the substrate and a nitrogen site that is active toward  $\text{CO}_2$  adsorption. In this work, the species grafted on the surface of the solid will be referred to as a tether and differs in chemical composition from the parent chemical because the methoxy moieties are lost during the condensation reaction.

Previous work has identified chemically stable, siliceous materials such as SBA-15 and silica gel as substrates for the tethers.<sup>17–21</sup> Such amorphous metal oxides are well-suited for chemical grafting as, unlike crystalline materials, all of the surface-exposed atoms terminate in hydroxyl groups. This allows a high density of tethers to be exposed along the pore walls. Work has also been done exploring amine functionalization of zeolitic materials including FAU/EMT,<sup>22</sup> ITQ-6,<sup>23</sup> and MFI.<sup>24</sup> FAU/EMT is the IZA (International Zeolite Association) framework identifier for a specific zeolite structure, ITQ-6 is the IZA (International Zeolite Association) framework identifier for a specific zeolite structure, and MFI is the IZA (International Zeolite Association) framework identifier for a specific zeolite structure. To date, all previous materials studied have been porous substrates due to the enhanced surface area and tether loading that comes with such materials. A risk lies with porous materials, however, because pore systems can concentrate nontarget gases and vapors. This characteristic makes porous materials prone to process upset when exposed to very high humidity, mist, or a slug of liquid that moves through the system.

This work focuses on functionalizing the surface of Engelhard titanasilicate 2 (ETS-2), a sodium nanotitanate. ETS-2 first described in a 1989 patent<sup>25</sup> is somewhat misnamed. ETS-2 is a form of sodium titanate which, through the addition of silica to the synthesis hydrogel, forms nanometer sized particles whose surfaces are covered in sodium titanate, an effective ion-exchanger. The small size of these nanotitanate particles gives them a high surface area ( $\sim 300 \text{ m}^2/\text{g}$ ) with no porosity, meaning that these adsorbents will resist fouling conditions capable of deactivating porous materials. The surface of ETS-2 also contains a high concentration of free hydroxyl groups, making ETS-2 an attractive support for aminosilane grafting and the lack of porosity places eliminates restrictions on the size of amine tethers which can be grafted to the surface of the substrate.

In this study, a series of aminosilanes was grafted to as-synthesized ETS-2. Aminosilanes containing one, two, and three amine groups were grafted to the surface of ETS-2. The thermal stability of the tethers was assessed using TG-MS under both inert and oxidizing atmospheres. The TG-MS data was also used to assess the capacity of the various sam-

ples toward trace amounts of  $\text{CO}_2$  in humid air. The adsorption capacities of the grafted amines were assessed using pure gas  $\text{CO}_2$  isotherms collected at 30, 50, and  $70^\circ\text{C}$  using a static volumetric adsorption system. Gravimetric adsorption cycling experiments under dry  $\text{CO}_2$  were carried out to assess each materials approach to cyclic steady state.

## Experimental

The ETS-2 samples used were synthesized hydrothermally using a previously published procedure.<sup>25</sup> Samples of ETS-2 (1.0 g) were combined with 28 mmol of aminosilane in a round bottomed flask. Figure 1 shows a schematic of the grafting reaction. Approximately 75 mL of toluene was added and the mixture was heated under reflux using a heating mantle for 6 h. Following this reflux, the samples were filtered and washed with toluene and then washed with deionized water. The samples were then dried in an oven at  $80^\circ\text{C}$  before being transferred to tightly capped glass vials.

Aminosilane reagents were reacted with samples of ETS-2, grafting the organic functions to the substrate using a siloxane bond. The aminosilane molecules used in this study were (3-Aminopropyl)trimethoxysilane (Sigma Aldrich), [3-(2-Aminoethylamino) propyl]trimethoxysilane (Sigma Aldrich), and N 1-(3-Trimethoxysilylpropyl) diethylenetriamine (Sigma Aldrich). These molecules are further referred to as N1, N2, and N3, respectively, in reference to the number of amine groups present in the molecule and the resulting grafted samples are designated N1-ETS-2, N2-ETS-2, and N3-ETS-3, respectively.

## TG-MS

The TG-MS plots were collected using a TA Instruments Q500 thermogravimetric analysis (TGA) coupled to a Pfeiffer Omnistar QMA 200 residual gas analyzer. TG scans were run using a balance purge rate of 40 mL/min  $\text{N}_2$  and a sample purge rate of 150 mL/min. The sample purge gas was selected from  $\text{N}_2$  or dry, compressed air depending on the sequence being run. Samples were loaded on platinum pans and heated at a rate of  $10^\circ/\text{min}$  from ambient to  $600^\circ\text{C}$ .

The mass spectrometer was configured with a stainless steel capillary heated to  $200^\circ\text{C}$  and connected to the TGA by means of a stainless steel adapter and a  $1/4''$  branch T-fitting. The capillary was positioned at the center of the tee close to the furnace exhaust to sample the evolved gases. The exhaust end of the T-fitting was connected to a 6 m length of  $1/4''$  OD tubing that prevented back-diffusion of atmospheric components and led to a fume hood exhaust. Experiments were run in MID mode with fragments at  $m/z = 15$ , 18, and 44 tracked over time. These fragments were found to be the most diagnostic signals associated with the decomposition of the tethers. To start data collection, the two

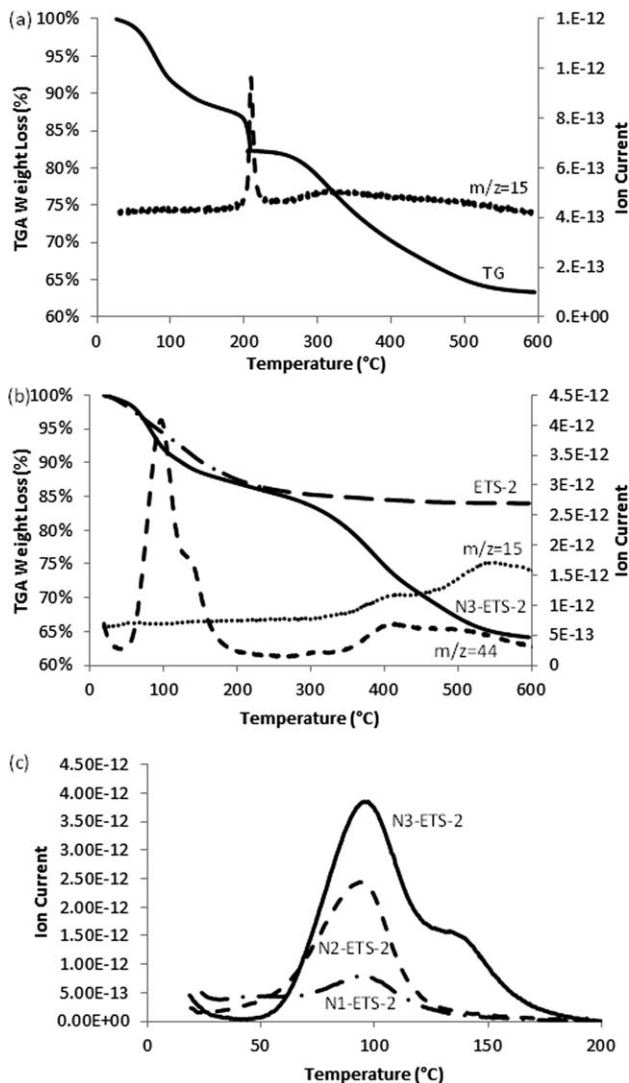


**Figure 2.** (a) TG-MS plot for the calcination of N3-ETS-2 in air. (b) TG-MS plots for N3-ETS-2 under N<sub>2</sub> with the TG plot of ETS-2 shown for reference. (c) MS plots at  $m/z = 44$  for N1-, N2-, and N3-ETS-2 heated under N<sub>2</sub>.

instruments were manually synchronized and an uncertainty of a few tenths of a degree for the starting temperature can be expected between the TG and MS plots.

#### Static volumetric adsorption

CO<sub>2</sub> isotherms were collected on a Micromeritics ASAP 2020C surface area and porosity analyzer. Isotherms were collected using the chemisorption function and the sample furnace. Samples (~250 mg) were packed into quartz tubes containing a 1-cm plug of quartz wool in the bottom. Samples were activated *in situ* under a flow of N<sub>2</sub> (~200 mL/min) using a ramp rate of 10°/min and were held under flow at 200°C for 15 min. The N<sub>2</sub> flow was then stopped and the sample evacuated for 60 min at 200°C. Samples were cooled, under vacuum (0.3 Pa), to their analysis temperature and isotherms were collected in fixed dosing mode with an equilibration delay of 5 s. Some replicate experiments were carried and it was found that the adsorption capacities were fully reproducible which suggests that the tethers are entirely stable at 200°C under hard vacuum.

#### Adsorption/desorption cycles

Adsorption/desorption cycles were collected by sequencing a series of activation and adsorption steps. The same TA Instruments Q500 instrumentation was used as for the TG-MS experiments. To achieve equal volumetric flow rates for N<sub>2</sub> and CO<sub>2</sub> the TG instrument setpoints were determined using an Agilent ADM 1000 volumetric flow meter connected to the exhaust of the furnace. This step was necessary as the TG instruments flow controllers were not calibrated for CO<sub>2</sub> and if the same setpoint was used for both gases then the measured flows differed substantially. Careful matching of the flow rates is important because a large difference in flow rate will change the force on the sample pan and an artificial weight change will be registered when the instrument switches from one gas to another. The tuned analysis protocol was tried on a sample of ground quartz wool and it was determined that, after the flow rates were properly matched, the switching event did not cause a measurable deflection in the baseline signal.

The flow values in brackets correspond to the instrument setpoint values. Samples were equilibrated at 40°C and then heated at 20°/min to 150°C under N<sub>2</sub> (40 mL balance purge, 118 mL/min sample purge). An isothermal dwell of 20 min at 150°C was followed by a cooling step to 70°C. After an isothermal dwell of 5 min at 70°C, the sample purge gas was switched to CO<sub>2</sub> (200 mL/min) and the sample equilibrated for 20 min. The CO<sub>2</sub> was desorbed by switching the sample gas back to N<sub>2</sub> and heating the sample to 150°C under the same conditions as previous. A total of 20 of these sequences was carried out for each sample.

## Results and Discussion

#### Air TG-MS

To quantify the amount of grafted material on ETS-2, samples were calcined in air to completely remove the organic material from the surface of the nanotitanate. The MS plots were used to indicate the onset of decomposition of the tether which was unique for each adsorbent.

Figure 2a shows the decomposition, in air, of N3-ETS-2. The signal at  $m/z = 15$  was used to determine the onset of decomposition because the fragment is specific toward the aminosilane decomposition and is unaffected by water or any of the components in air. The obvious spike in the MS plot and corresponding step change in the TG plot is characteristic of a combustion event as neither of these features were evident in subsequent scans under a N<sub>2</sub> atmosphere.

The quantification of the number of moles of tether per gram of substrate required a number of influences to be taken into account. The TG experiment will only combust the organic fraction of the tether and the silicon atom will be left behind on the substrate. This influences both the calculation of the mass of the tether and the mass of the substrate. Another complication is that the substrate will continue to sinter and evolve water as the temperature is increased and so the total mass loss is a combination of combusted material and water loss from the substrate.

To calculate the weight loss due to the combustion of the tether, the onset of combustion was determined for each sample from the TG-MS plots. The onset temperatures and onset weights for the adsorbents were taken at 275°C for N1-ETS-2, 200°C for N2-ETS-2, and 190°C for N3-ETS-2. The total weight loss between the onset temperature and 600°C was calculated for each sample from their respective TG plots. As

**Table 1. Values Used in the Calculation of the Mass of Aminosilane on ETS-2**

	FW with Si (g/mol)	FW without Si (g/mol)	Onset Wt <sup>a</sup> (mg)	600°C Wt (Mg)	Water Loss (mg)	Net Loss (mg)	Si-Adjusted Net Loss (Mg)	Aminosilane (Mol)	Aminosilane (G)	Wt Ratio (%)	Wt Fraction (%)
<b>N1</b>	86.17	58.09	40.21	35.06	0.68	4.47	6.63	5.19E-05	4.47E-03	12.50	11.10
<b>N2</b>	129.24	101.16	38.70	29.80	1.25	7.64	9.76	5.91E-05	7.64E-03	24.60	19.80
<b>N3</b>	172.31	144.23	35.58	23.65	1.14	10.79	12.90	6.26E-05	1.08E-02	43.60	30.30

<sup>a</sup>The weight at which tether decomposition begins.

mentioned above, the total weight loss is a combination of the removal of the combustible portion of the aminosilane tether as well as water lost from the substrate.

The weight loss due to water between the various onset temperatures and 600°C was calculated using a TG plot for raw ETS-2. Although it might be considered that the grafting procedure would remove surface hydroxyls that would condense at higher temperatures, the MS signal at  $m/z = 18$  for the tethered samples shows continual emission of water from the solid as the material is heated. The rise, at elevated temperatures, in the intensity of the signal at  $m/z = 18$  was confirmed in subsequent experiments run under dry  $N_2$  which confirmed that the solid is dehydrating at elevated temperatures. The fraction of water lost between the various onset temperatures and 600°C for raw ETS-2 was calculated from the TG plot and then scaled to the individual grafted samples' weight at each of their onset temperatures. Water loss accounted for about 10% of the total mass loss for the grafted samples and thus should be factored out to prevent this effect from skewing the calculations of amine loading. The net loss, used for all subsequent analyses, was calculated by subtracting the weight loss due to water from the total mass lost for each adsorbents unique temperature range.

The various formula weights used in the assessment of the mass loading of the tethers were arrived at by factoring in only the chemical groups relevant to the calculation. The molecular weight of the aminosilane tether was calculated by subtracting the three methoxy groups on the original trimethoxyaminosilane reagent because these groups should be lost as methanol during the grafting process. The aminosilane tether is thus the  $C_xH_yN_z$  (CHN refers to the specific atomic components of the tether materials) chain including a single silicon atom. Any oxygen associated with the grafting would have come from the substrate and are, therefore, not accounted for in the calculation of the tether formula weight. The molecular weight of the combustible tether is simply the formula weight of the aminosilane tether less than the silicon atom.

The moles of combustible tether were converted to moles of aminosilane tether by scaling the moles of amine chain lost in the TG experiment back to aminosilane by way of their respective formula weights. To determine the weight ratio of aminosilane on the substrate, the mass of silicon remaining on the calcined sample must first be subtracted from the residual mass of the sample. This was accomplished by calculating the

number of grams of silicon present in the same number of moles of combustible tether. The contribution of the silicon to the substrate mass at 600°C is significant, being on the order of 5–6% of the total sample mass.

The values provided in Table 1 provide the sequence of values used in the calculations. The term "AS" refers to the aminosilane tether, including the silicon atom. The weight ratio of the aminosilane is the ratio of the mass of aminosilane vs. the mass of the bare substrate. The weight fraction is defined as the mass of the aminosilane over the total sample weight (including the tether). The weight ratio scales linearly with the formula weight of the aminosilane though the correlation coefficient suggests that the loading of the amine on each sample is not equivalent for all samples.

Using the measured surface area of the substrate and the aminosilane molecular cross section ( $5 \times 10^{18}$  molecules/m<sup>2</sup>)<sup>26</sup> the aminosilane weight ratio can be calculated at monolayer coverage. Table 2 gives the values used in the calculations and the expected tether weight ratios at monolayer coverage for ETS-2. The calculated aminosilane weight ratio at monolayer coverage is higher than the measured values for the N1 and N2 samples but quite close to the measured value in the case of the N3 sample. The same molecular cross sectional area can be used to calculate the surface area of the substrate covered by the measured amount of grafted material. The data in Table 2 shows that there is an increasing trend in the calculated degree of surface coverage moving from the N1 sample to the N3 sample. Comparing the measured surface area data with the calculated surface coverage, it can be determined that the N1 sample is likely 60% covered, the N2 sample 80% covered, and the N3 sample is completely covered with aminosilane tethers. Steric arguments cannot explain why the larger aminosilane provides a higher surface coverage so it is assumed that further synthesis optimization should allow all samples to converge on 100% surface coverage.

## ***N<sub>2</sub> TG-MS***

TG-MS scans were run under  $N_2$  to determine the onset decomposition temperature for the tethers in a nonoxidizing atmosphere. All of the MS scans showed an interesting and unexpected feature at low temperature at  $m/z = 44$ . The magnitude of the signals and trends between samples were similarly seen in the air TG-MS data when that signal was examined. Further analysis was done on the  $N_2$  TG-MS data

**Table 2. Values Used in the Calculation of the Weight Ratio and Surface Area Coverage of the Tethers**

Sample	Measured Surface Area (m <sup>2</sup> /g)	Estimated at Monolayer Coverage AS Weight Ratio (g/g)	Measured AS Wt Ratio (g/g)	Calculated Surface Area (m <sup>2</sup> /g)
<b>N1</b>	290	20.74%	12.51%	175
<b>N2</b>	290	31.11%	24.61%	229
<b>N3</b>	300 <sup>a</sup>	42.91%	43.55%	304

<sup>a</sup>Sample N3 was prepared using a different batch of base material having a slightly different surface area.



**Table 3. Values Used in the Calculation of the Amount of CO<sub>2</sub> Adsorbed Per Mole of Aminosilane**

	FW (g/mol)	Wt fraction AS (%)	Onset Sample Mass <sup>a</sup> (mg)	Aminosilane (mg)	Aminosilane (mmol)	Integrated CO <sub>2</sub> Intensity (arb.units)	CO <sub>2</sub> /mmol AS	Normalized Ratio
N1	86.17	11.12	25.04	2.78	3.23E-02	4.55E-11	1.41E-09	1.00
N2	129.24	19.75	31.85	6.29	4.87E-02	9.18E-11	1.89E-09	1.34
N3	172.31	30.34	24.17	7.33	4.26E-02	3.56E-10	8.37E-09	5.95

<sup>a</sup>Sample mass when tether decomposition begins.

to eliminate the influence of any contamination present in the air stream. Figure 2b shows the N<sub>2</sub> TG-MS plot for N3-ETS-2 with the corresponding MS signals at  $m/z = 15$  and 44. The TG plot for raw ETS-2 is overlaid for reference.

The difference in the two TG plots is evident in that the N3-ETS-2 sample contains two transitions absent in the substrate. The signal at  $m/z = 15$  indicates that the weight loss above 300°C is due to the decomposition of the tether. This result also demonstrates the enhanced thermal stability of the grafted samples under anoxic conditions as the onset decomposition temperature is shifted from 200 to 300°C. The thermal stability of the amine tethers in both air and N<sub>2</sub> appears sufficient for long-term process stability. The regeneration temperature for CO<sub>2</sub> desorption in a packed bed system is expected to not exceed 200°C as this is the temperature at which the amine reboilers are maintained to flash off the adsorbed CO<sub>2</sub>. To be competitive, a packed bed system should work within the conventional temperature envelop for amine systems and thus regeneration temperatures in excess of 200°C are not considered.

The low-temperature TG transition centered on about 100°C is assigned to CO<sub>2</sub> desorption from the material. This assignment can be made unambiguous because there is no sign of pyrolysis of the tethers at low temperature (evidenced by the signal at  $m/z = 15$ ) and the analysis system (under N<sub>2</sub>) has nondetectable levels of CO<sub>2</sub> and hydrocarbons that appear at  $m/z = 44$ . The CO<sub>2</sub> adsorption on the samples was entirely voluntary as the samples were not pretreated or preconditioned in any way prior to analysis. The observation of CO<sub>2</sub> on the adsorbents suggests the performance of these materials will be unaffected by moisture as the moisture concentration in the lab, while not monitored, is expected to be at least an order of magnitude greater than the ~400 ppm of CO<sub>2</sub> present.

The adsorption capacity of the various materials can be assessed by integrating the signal at  $m/z = 44$ . To maintain a fair comparison, all of the plots were reduced to a common baseline to prevent run-to-run baseline offset from influencing the analysis. The MS traces at  $m/z = 44$  were integrated between 30 and 200°C and these integrated ion currents represent the mass of CO<sub>2</sub> adsorbed on the solid. The upper limit of 200°C was chosen because this was identified as the highest common temperature at which there was no evidence of tether decomposition and at which the majority of the CO<sub>2</sub> had been desorbed from the sample. Figure 2c shows the overlay of the MS scans at  $m/z = 44$  for the N1, N2, and N3 samples that have been adjusted by subtracting each samples initial CO<sub>2</sub> ion current from their respective raw signal values.

The amount of CO<sub>2</sub> (in arbitrary units) can be standardized by the moles of aminosilane in each sample. Table 3 shows the sequence of values used in the calculations. The aminosilane weight fractions calculated from the air TG-MS data can be applied to the sample weights taken from the N<sub>2</sub> TG-MS plots at 200°C and the moles of aminosilane can subsequently be calculated for each sample. Dividing the integrated CO<sub>2</sub> signal by the corresponding molar quantity

of aminosilane yields a standardized quantity that factors out the varying sample weights used in the experiments.

The relative performance of the adsorbents can be gauged by normalizing the standardized values against the N1 sample. Table 3 shows the trend in the normalized value for relative CO<sub>2</sub> capacity and it is evident that the N3 material has significantly higher capacity compared to the other two samples. This result was unanticipated as the N3 tether is predominantly secondary amines which are not as reactive as primary amines. The humidity present in ambient air will, however, allow the secondary amines to participate in CO<sub>2</sub> adsorption and causing the CO<sub>2</sub> capacity to scale linearly with the number of amine groups on the tether. The nonlinear behavior of the trend can be explained by taking into account the degree of monolayer coverage for each sample. The 2:1 stoichiometry for CO<sub>2</sub> adsorption in amine systems requires the CO<sub>2</sub> to interact with two amine groups. It is considered that the higher degree of surface coverage and the higher density of nitrogen groups lends the N3 sample a significant advantage compared to the two other samples with lower surface coverage. The presence of a second peak, at higher temperature, in the trace for the N3 sample in Figure 2c, establishes the greater adsorption strength for the N3 sample as none of the other sample show similar behavior though, chemically, the tethers are all comparable. The differences between the samples suggest that the adsorptive performance of grafted, nonporous adsorbents is significantly affected by the degree of surface coverage of the tether.

### Adsorption isotherms

The CO<sub>2</sub> isotherms at 30°C for the three amine samples are shown in Figure 3. There is little differentiation between samples at 30°C though the N1 material has a marginally higher capacity. This could be expected given that the N1 material is comprised entirely of primary amine groups which are more reactive toward CO<sub>2</sub> compared to secondary and tertiary amines.<sup>18</sup> Kinetic influences could also contribute to this trend because the activation barrier for the

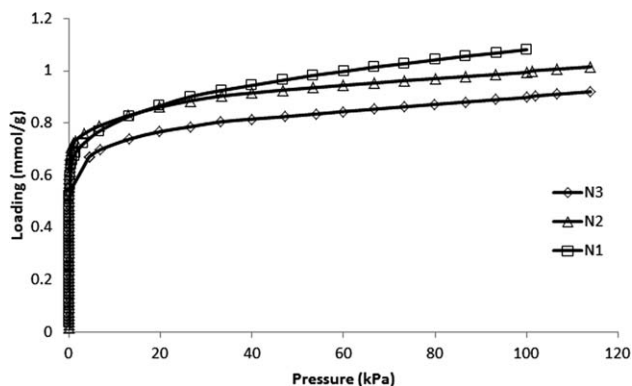


**Figure 3. CO<sub>2</sub> adsorption at 30°C for aminosilane grafted ETS-2.**

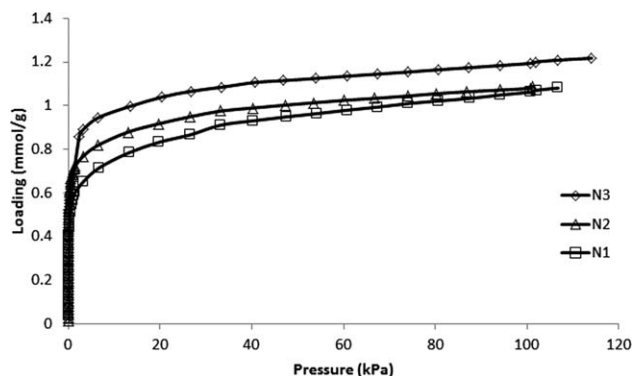


Figure 4. CO<sub>2</sub> adsorption at 50°C for aminosilane grafted ETS-2.

reaction of the CO<sub>2</sub> with the amines is not expected to be overcome easily at 30°C.<sup>27,28</sup> Kinetic effects can be expected as the equilibration delay used in the analyses is typical of small molecule adsorption on molecular sieves and will be biased against a slow approach to equilibrium. It should also be considered that all of the adsorption experiments presented are run under rigorously anhydrous conditions and thus the amines cannot take advantage of moisture acting as a promoter to form carbamate ions.<sup>29–31</sup> The presence of a promoter could change the adsorption characteristics and/or rates compared to the data presented.

At 50°C, the CO<sub>2</sub> isotherms (Figure 4) begin to show a trend with respect to the number of amines on the tether and at 70°C (Figure 5), there is a clear differentiation between the various samples. Figure 6 also includes the CO<sub>2</sub> isotherm for the raw ETS-2 substrate. The ETS-2 substrate demonstrates an affinity for CO<sub>2</sub> and the isotherm is well described by the Toth equation suggesting strong physisorption. Isotherms for the substrate were collected at 30, 50, and 70°C and the isosteric heat of adsorption calculated for CO<sub>2</sub> on raw Na-ETS-2 exceeds 30 kJ/mol at loadings less than 0.6 mmol/g and exceeds 40 kJ/mol at loadings below 0.3 mmol/g. At low partial pressures, however, the adsorption characteristics of the tethered samples are obviously directed by the chemistry of the tether because the CO<sub>2</sub> isotherm for the substrate lacks the rectangularity seen in the tethered samples. The progressive increase in capacity with CO<sub>2</sub> partial pressure for the tethered samples could be due to the gas interacting with the substrate because the specificity of the amine-CO<sub>2</sub> interaction does not predict a rise in capacity with increasing partial pressure.

At 70°C kinetic effects should be minimized due to the greater amount of thermal energy in the gas molecules and,

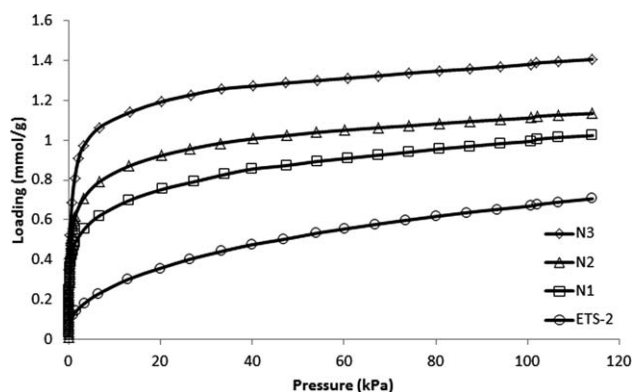


Figure 5. CO<sub>2</sub> adsorption at 70°C for aminosilane grafted ETS-2.

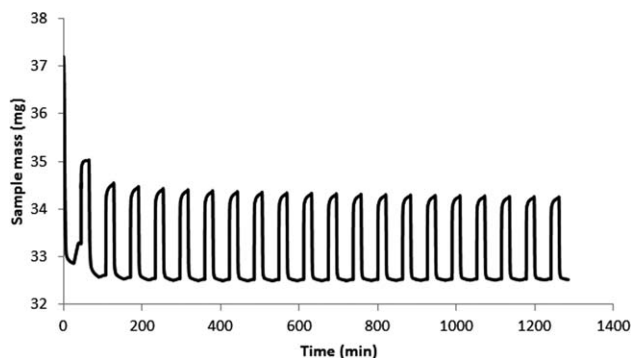


Figure 6. TG plot for CO<sub>2</sub> adsorption/desorption cycling on N3-ETS-2.

at this temperature, it is reasonable to assume that activation barriers are largely overcome. The comparison of the adsorption capacity of the adsorbents used the 70°C isotherms because it was felt that these isotherms were the least influenced by equilibrium effects. A similar analysis that was done using the N<sub>2</sub> TG-MS data can be done using adsorption data at 70°C. The capacity at 50 kPa was selected as the point of comparison because this represents a likely upper limit in the partial pressure of CO<sub>2</sub> that might be encountered in a flue gas cleanup process. The central pressure in the isotherm also limits the bias due to the contribution from the substrate to the overall capacity of the sample. The adsorption data at 50 kPa in mmol/g was converted to express the capacity of the adsorbent as moles of CO<sub>2</sub> adsorbed per mole of aminosilane. The same aminosilane weight fractions and formula weights used in analysis of the N<sub>2</sub> TG-MS data were used in the analysis of the volumetric adsorption data.

Table 4 shows the values used in the calculations and the results of the comparison. When the moles of CO<sub>2</sub> adsorbed are standardized against the number of moles of aminosilane, it becomes apparent that the adsorptive capacity for all of the samples is roughly equivalent. A slight upward trend from the N1 to the N3 sample can be noted but the increase does not scale with the number of amines on the chain. Normalizing these ratios against the N1 sample, it becomes clear that the secondary amines are not likely involved in CO<sub>2</sub> adsorption under the experimental conditions.

This result is reasonable as it is known that only primary amines have a facile reaction with CO<sub>2</sub> in the absence of water vapor and the activation condition for the samples effectively excluded all water vapor from the system. The slight increase in the normalized ratio between the N1 and N3 samples could be due to the primary amines having a marginally higher degree of efficiency on the N3 sample due to the higher degree of surface coverage. Although the trend between the samples suggests a shift in amine efficiency, the magnitude of the difference should be considered semiquantitative until the combined uncertainty of all measurement systems coupled with the sample-to-sample variability can be established. The N<sub>2</sub> TG-MS data showed a clear enhancement in CO<sub>2</sub> capacity for the N3 sample while the volumetric adsorption data indicates the performance of all tethers is comparable once the number of moles of tether on each adsorbent is accounted for. The contrast between the relative efficiencies of the adsorbents between datasets confirms the importance of water as a promoter in these materials.

**Table 4. Values Used in the Normalization of 70°C Volumetric Adsorption Data**

	FW AS	Weight Fraction AS (%)	CO <sub>2</sub> Capacity at 50 kPa (mmol/g)	mol CO <sub>2</sub> /g AS	mol/mol (CO <sub>2</sub> /AS)	Normalized
N1	86.17	11.10	0.87	7.82E-03	0.67	1.00
N2	129.24	19.80	1.04	5.27E-03	0.68	1.01
N3	172.31	30.30	1.30	4.29E-03	0.74	1.10

### Adsorption cycling

Adsorptive cycling experiments were performed to examine the approach of the adsorbents to cyclic steady state under nonequilibrium conditions. The CO<sub>2</sub> capacity for the adsorbents is not quantified using this data because of the uncertainty attached to the partial pressure CO<sub>2</sub> used in the experiment. It can be assumed that the purge gas is mixed with the balance gas to create a stream that is a perfect blend of the two but the mixing dynamics in the instrument are not known and this assumption may not be reliable. The instrument operation, however, is expected to be consistent for each cycle and each sample. As such, the trends seen in the data are considered quantitative, whereas the CO<sub>2</sub> uptake values are semiquantitative.

An example of the adsorption cycling for the N3-ETS-2 sample is shown in Figure 7 where it can be seen that the sample does not equilibrate with CO<sub>2</sub> within time allotted. This result is common for all of the tethered samples and could be due to the anhydrous condition of the test which favors the primary amine on the tether or it could be due to system dynamics where the atmosphere within the instrument is not equilibrated within the given 20 min period. Rather than invest in additional equilibration time, it was elected to run additional cycles to map the approach of the samples to cyclic steady state.

The weight change for each cycle was measured from the plateau at 70°C under N<sub>2</sub> (just before the sample purge gas was switched to CO<sub>2</sub>) until the end of the 20 min isothermal delay used for CO<sub>2</sub> adsorption. To confirm the stability of the measurement, the amount of CO<sub>2</sub> adsorbed and desorbed for each cycle was measured. The amount of mass gained during CO<sub>2</sub> adsorption was equal to the amount lost during regeneration within a hundredth of a milligram which is well within the uncertainty of the measurement.

The mass change during CO<sub>2</sub> adsorption was standardized using the moles of aminosilane present on the sample. The moles of aminosilane on each sample were calculated by

applying the respective weight fraction for each tether to the sample mass measured before the final adsorption step. The same analysis was done using the sample mass measured before the first CO<sub>2</sub> adsorption and the results are indistinguishable. From Figure 7, it is apparent that the three samples initially have roughly the same CO<sub>2</sub> loading per mole of aminosilane. This was expected as the CO<sub>2</sub> isotherm data demonstrated that the adsorption capacity of the three samples, under dry conditions, should be roughly equivalent when the adsorption capacity is standardized by the number of moles of amine on the support. As additional cycles are run, the samples begin to distinguish themselves in their approach to steady state. Although the N1 sample shows a relatively steep downward trend the N3 sample appears to be trending to steady state toward the end of the 20 cycles. The N2 sample displays behavior somewhere between the other two samples; dropping capacity as a function of cycle time yet not at the same rate as the N1 sample.

The gradual loss in capacity is not likely due to the degradation of the tethers as all previous experiments have demonstrated that the tethers are thermally stable toward the selected regeneration temperature. Likewise, the substrate is not expected to be contributing to this behavior as a sample of Na-ETS-2 was analyzed using the same protocol and the sample reached cyclic steady state within 10 cycles and displayed a loss of less than a percent over the span of cycles (Figure 8). It is probable that the cycle chosen, combined with the experimental conditions, are preventing the samples from equilibrating within the given cycle and that 20 cycles may not be sufficient to achieve cyclic steady state under anhydrous conditions.

It is not clear why the downward trend in capacity is not associated with any gain, or loss, in sample mass. It was measured that each cycle is completely reversible and that the activated sample mass does not fluctuate from cycle to cycle. The cyclic losses are thus not apparently due to accumulation of CO<sub>2</sub> on the solid nor are they due to the cumulative loss of some necessary component from the sample. It is proposed that the adsorption of CO<sub>2</sub> on such composite

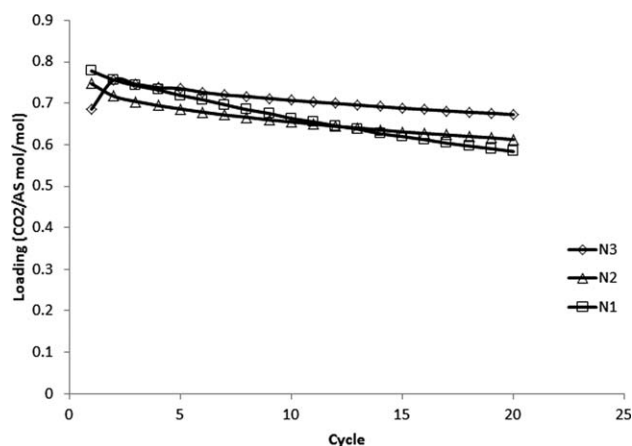


**Figure 7. Cyclic CO<sub>2</sub> capacity for aminosilane grafted ETS-2.**

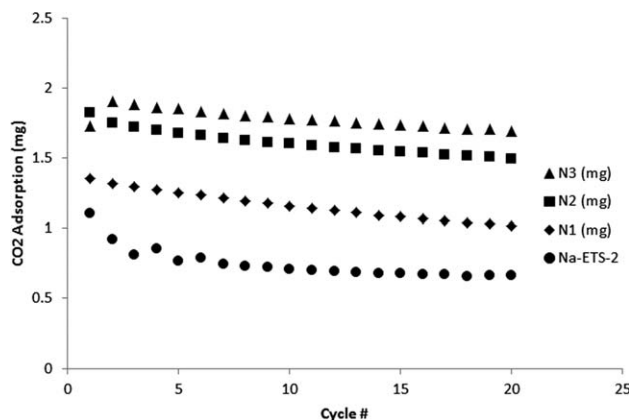


**Figure 8. Gravimetric uptake of CO<sub>2</sub> for grafted and ungrafted ETS-2.**



adsorbents under the test conditions is not well enough understood to provide a clear mechanism to explain the measured behavior. It is anticipated, however, that the same tests run under humid conditions should provide the conditions necessary for the amines, and particularly the secondary amines, to behave in a manner which mirrors the accepted mechanisms for CO<sub>2</sub> adsorption.

The degree of aminosilane surface coverage could influence the rate at which the samples can adsorb CO<sub>2</sub>. The closer proximity of the tethers in the N3 sample should provide a more uniform adsorption field and the close packing of the tethers should facilitate the stoichiometry needed for carbamate formation. In the N1 and N2 samples, the tethers should be further apart, on average, which should create a barrier to reaction. A sensitivity to the degree of monolayer coverage is reasonable for these samples as ETS-2 cannot take advantage of pore amplification effects where the pore system of the substrate can locally concentrate components and thus facilitate reaction with the amine functions on the tether.

## Conclusions

The first series of nonporous, amine-grafted nanotitanates was prepared using a range of aminosilanes containing up to three amine groups on the chain. The N3-ETS-2 sample was shown through TG-MS to have five times the capacity of the N1 sample for removing trace-levels of CO<sub>2</sub> from ambient air. The adsorption results demonstrated that anhydrous adsorption conditions favor the primary amines and that the benefits of having multiple amine groups on the tether are not measurable under such test conditions. The nonporous nanotitanates are considered to be sensitive to the degree of aminosilane monolayer coverage and that enhanced capacity and adsorption rates can be realized when the aminosilane density approaches monolayer coverage of the substrate. This behavior may be unique to high surface area, nonporous substrates because they cannot take advantage of pore amplification effects where the pore system of the substrate can locally concentrate gases or vapor and thus facilitate reaction with the amine.

## Acknowledgments

The authors gratefully acknowledge the research funding provided by the Helmholtz-Alberta Initiative (HAI), Carbon Management Canada, and Canada Research Chair in New Molecular Sieves (SMK).

## Literature Cited

- United Nations Statistics Division, Carbon dioxide emissions (CO<sub>2</sub>) thousand metric tons of CO<sub>2</sub> (CDIAC). *UNData*. 2012. Available at [http://data.un.org/Data.aspx?q=Carbon+dioxide+emissions+\(per+capita\)+CFCs&d=MDG&f=seriesRowID%3a749](http://data.un.org/Data.aspx?q=Carbon+dioxide+emissions+(per+capita)+CFCs&d=MDG&f=seriesRowID%3a749). Last accessed: Jan. 15, 2013.
- Drage TC, Smith KM, Pevida C, Arenillas A, Snape CE. Development of adsorbent materials for post-combustion CO<sub>2</sub> capture. *Energy Procedia*. 2009;1:881–884.
- Hwang K-S, Son Y-S, Park S-W, Park D-W, Oh K-J, Kim S-S. Adsorption of carbon dioxide onto EDA-CP-MS41. *Sep Sci Technol*. 2010;45:85–93.
- Park SW, Yun YH, Kim SD, Yang ST, Ahn WS, Seo G, Kim WJ. CO<sub>2</sub> retention ability on alkali cation exchanged titanium silicate, ETS-10. *J Porous Mater*. 2010;17:589–595.
- Zhao Z, Cui X, Ma J, Li R. Adsorption of carbon dioxide on alkali-modified zeolite 13X adsorbents. *Int J Greenhouse Gas Control*. 2007;1:355–359.
- Areal CO, Delgado MR. Variable-temperature FT-IR studies on the thermodynamics of carbon dioxide adsorption on a faujasite-type zeolite. *Appl Surf Sci*. 2010;256:5259–5262.
- Zukal A, Mayerova J, Kubu M. Adsorption of carbon dioxide on high-silica zeolites with different framework topology. *Top Catal*. 2010;53:1361–1366.
- Konduru N, Lindner P, Assaf-Anid NM. Curbing the greenhouse effect by carbon dioxide adsorption with Zeolite 13X. *AIChE J*. 2007;53(12):3137–3143.
- An H, Feng B, Su S. CO<sub>2</sub> capture by electrothermal swing adsorption with activated carbon fibre materials. *Int J Greenhouse Gas Control*. 2011;5(1):16–25.
- Arenillas A, Smith KM, Drage TC, Snape CE. CO<sub>2</sub> capture using some fly ash-derived carbon materials. *Fuel*. 2005;84(17):2204–2210.
- Goodman AL. A comparison study of carbon dioxide adsorption on polydimethylsiloxane, silica gel, and illinois no. 6 coal using in situ infrared spectroscopy. *Energy Fuels*. 2009;23(2):1101–1106.
- Witton T, Tatan N, Rattanavichian P, Chareonpanich M. Preparation of silica xerogel with high silanol content from sodium silicate and its application as CO<sub>2</sub> adsorbent. *Ceram Int*. 2011;37(7):2297–2303.
- Chen C, Ahn W-S. CO<sub>2</sub> capture using mesoporous alumina prepared by a sol-gel process. *Chem Eng J*. 2011;166(2):646–651.
- Li M. Dynamics of CO<sub>2</sub> adsorption on sodium oxide promoted alumina in a packed-bed reactor. *Chem Eng Sci*. 2011;66(23):5938–5944.
- Chatti R, Banswal AK, Thote JA, Kumar V, Jadhav P, Lokhande SK, Biniwale RB, Labhsetwar NK, Rayalu SS. Amine loaded zeolites for carbon dioxide capture: amine loading and adsorption studies. *Micropor Mesopor Mater*. 2009;121:84–89.
- Jadhav PD, Chatti RV, Labhsetwar NK, Devotta S, Rayalu SS. Monoethanol amine modified zeolite 13X for CO<sub>2</sub> adsorption at different temperatures. *Energy Fuels*. 2007;21(6):3555–3559.
- Chang F-Y, Chao K-J, Cheng H-H, Tan C-S. Adsorption of CO<sub>2</sub> onto amine-grafted mesoporous silicas. *Sep Purif Technol*. 2009;70:87–95.
- Ko YG, Shin SS, Choi US. Primary, secondary, and tertiary amines for CO<sub>2</sub> capture: designing for mesoporous CO<sub>2</sub> adsorbents. *J Colloid Interface Sci*. 2011;361:594–602.
- Sakamoto Y, Nagata K, Yogo K, Yamada K. Preparation and CO<sub>2</sub> separation properties of amine-modified mesoporous silica membranes. *Micropor Mesopor Mater*. 2007;2007:303–311.
- Sayari A, Harlick PJE, Inventors. Functionalized adsorbent for removal of acid gases and use thereof. US patent, US 7,767,004 B2. August 3, 2010.
- Zhao Y, Shen Y, Bai L. Effect of chemical modification on carbon dioxide adsorption property of mesoporous silica. *J Colloid Interface Sci*. 2012;379:94–100.
- Nik OG, Chen XY, Kaliaguine S. Amine-functionalized zeolite FAU/EMT-polyimide mixed matrix membranes for CO<sub>2</sub>/CH<sub>4</sub> separation. *J Memb Sci*. 2011;379(1–2):468–478.
- Zukal A, Dominguez I, Mayerova J, Cejka J. Functionalization of delaminated zeolite ITQ-6 for the adsorption of carbon dioxide. *Langmuir*. 2009;25(17):10314–10321.
- Kassaei MH, Sholl DS, Nair S. Preparation and gas adsorption characteristics of zeolite MFI crystals with organic-functionalized interiors. *J Phys Chem C*. 2011;115(40):19640–19646.
- Kuznicki SM, Inventor. Large-pored crystalline titanium molecular sieve zeolites. US patent, US 4,853,202. August 1, 1989.
- Feng X, Fryxell GE, Wang L-Q, Kim AY, Liu J, Kemner KM. Functionalized monolayers on ordered mesoporous supports. *Science*. 1997;276:923–926.
- Monazam ER, Shadle LJ, Siriwardane R. Performance and kinetics of a solid amine sorbent for carbon dioxide removal. *Ind Eng Chem Res*. 2011;50:10989–10995.
- Ebner AD, Gray ML, Chisholm NG, Black QT, Mumford DD, Nicholson MA, Ritter JA. Suitability of a solid amine sorbent for CO<sub>2</sub> capture by pressure swing adsorption. *Ind Eng Chem Res*. 2011;50:5634–5641.
- Palmeri N, Cavallaro S, Bart JCJ. Carbon dioxide absorption by MEA-A preliminary evaluation of a bubbling column reactor. *J Therm Anal Calorim*. 2008;91:87–91.
- Park S-W, Lee J-W, Choi B-S, Lee J-W. Kinetics of absorption of carbon dioxide in monoethanolamine solutions of polar organic solvents. *J Ind Eng Chem*. 2005;11(2):202–209.
- Zelenak V, Halamova D, Gaberova L, Bloch E, Llewellyn P. Amine-modified SBA-12 mesoporous silica for carbon dioxide capture: effect of amine basicity on sorption properties. *Micropor Mesopor Mater*. 2008;116:389–364.

Manuscript received Apr. 18, 2013, and revision received Jun. 18, 2013.